

available at www.sciencedirect.comjournal homepage: www.elsevier.com/locate/biochempharm

Critical role of Bid and Bax in indirubin-3'-monoxime-induced apoptosis in human cancer cells

Jie Shi, Han-Ming Shen*

Department of Community, Occupational and Family Medicine, Yong Loo Lin School of Medicine, National University of Singapore, 16 Medical Drive, MD3, Singapore 117597, Republic of Singapore

ARTICLE INFO

Article history:

Received 9 November 2007

Accepted 24 January 2008

Keywords:

Indirubin-3'-monoxime

Death receptor

Bid

Bax

Apoptosis

ABSTRACT

Indirubin-3'-monoxime (I3M) is a derivative of indirubin, an active component from a Chinese medicinal recipe with known anti-cancer function. I3M has been well established as a cyclin-dependent kinase (CDK) inhibitor, while the molecular mechanism underlying I3M-induced apoptosis has not been fully elucidated. In this study, we focused on the critical role of the pro-apoptosis Bcl-2 family members in I3M-induced apoptosis. We first observed I3M-induced apoptosis in a time- and dose-dependent manner in three different types of human cancer cells—cervical cancer HeLa, hepatoma HepG2 and colon cancer HCT116. Induction of the caspase cascade for both the extrinsic and intrinsic pathways was demonstrated, including caspase-8, -9 and -3 activation. Initiation of the death receptor pathway started with enhanced surface expression of DR4 and DR5, as well as increased total protein level, which correlated with the up-regulation of p53 and its transcriptional activity. Importantly, we found in HeLa cells that caspase-8 activation resulted in Bid cleavage, followed by Bax conformational change and hence the amplification of the apoptotic signals through the mitochondrial pathway. Consistently, stable knockdown of Bid abrogated I3M-induced Bax conformational change and cell death. Moreover, ectopic expression of a viral caspase inhibitor (CrmA) or Bcl-2 partially protected I3M-induced apoptosis. In conclusion, our results indicate that I3M mainly elicits apoptosis through extrinsic pathway with type II response mediated by the pro-apoptotic Bcl-2 family members (Bid and Bax).

© 2008 Elsevier Inc. All rights reserved.

1. Introduction

Indirubin-3'-monoxime (I3M, Fig. 1A) is a derivative of indirubin which is the active component of Danggui-Long-Hui-Wan, a traditional Chinese recipe used for the treatment of various diseases in particular chronic myelogenous leukemia [1,2]. Indirubin and its derivatives, a group of bis-

indole alkaloids, have exhibited strong growth inhibitory effect on various human cancer cells, manifested by either cell cycle arrest (G2/M) [3,4] or cytotoxicity (mainly apoptosis) [4–7]. *In vivo* study carried out in rat tumor model provides further evidence for the anti-tumor activity of indirubins [8]. In the attempt to reveal the mechanism of action of indirubins, various biological activities of indirubin and its derivatives

* Corresponding author. Tel.: +65 6516 4998; fax: +65 6779 1489.

E-mail address: cofshm@nus.edu.sg (H.-M. Shen).

Abbreviations: I3M, indirubin-3'-monoxime; DAPI, 4',6-diamidino-2-phenylindole; MTT, thiazolyl blue tetrazolium bromide; PARP, poly(ADP-ribose)polymerase; z-VAD-FMK, z-Val-Ala-Asp(OMe)-fluoromethylketone; ac-DEVD-CHO, N-acetyl-Asp-Glu-Val-Asp-CHO (aldehyde); z-DEVD-FMK, z-Asp(OMe)-Glu(OMe)-Val-Asp; Ac-IETD-CHO, N-acetyl-Ile-Glu-Thr-Asp-CHO (aldehyde); Ac-LEHD-CHO, N-acetyl-Leu-Glu-His-Asp-CHO (aldehyde); PI, propidium iodide; CrmA, cytokine response member A; GFP, green fluorescence protein. 0006-2952/\$ – see front matter © 2008 Elsevier Inc. All rights reserved.

doi:10.1016/j.bcp.2008.01.021

have been discovered. It has been well established that indirubin and I3M are strong inhibitors of cyclin-dependent kinases (CDKs) [3,7]. In addition, there is evidence suggesting that indirubin and I3M inhibit glycogen synthase kinase-3 β (GSK-3 β) [9,10], and c-Src kinase (Stat3 signalling) [5], but activate aryl hydrocarbon receptor (AhR), a co-transcriptional

factor [11]. It was reported that indirubin could suppress the nuclear factor-kappa B (NF- κ B) activation and hence sensitize tumor necrosis factor (TNF)-induced apoptosis [12]. More recently, I3M has been found to inhibit autophosphorylation of FGFR1 and stimulates ERK1/2 activity through long-term p38 MAPK activation [13].

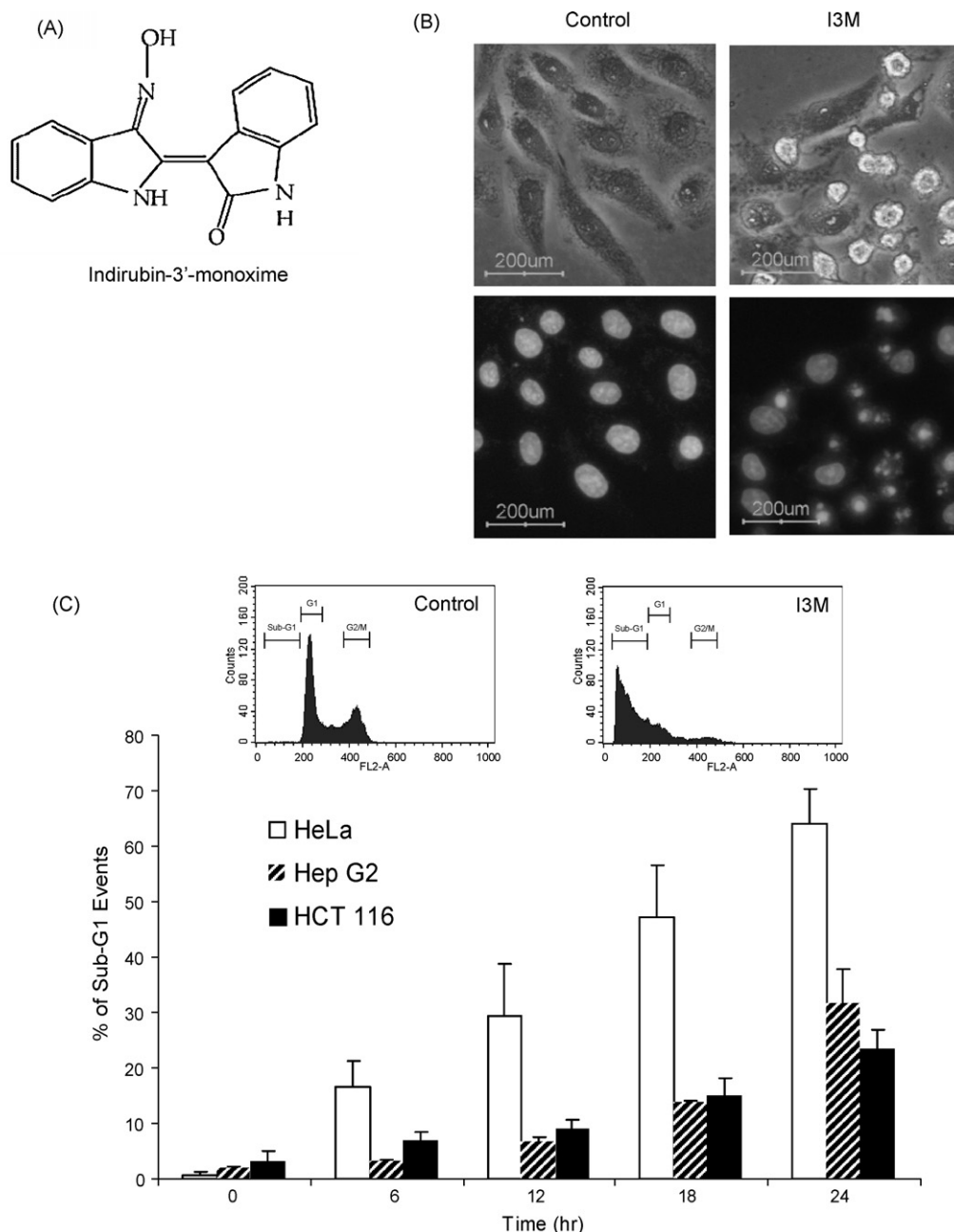


Fig. 1 – I3M-induced apoptosis in various human cancer cell lines. (A) The chemical structure of Indirubin-3'-monoxime [12]. **(B)** Typical morphological changes and nuclear condensation observed in I3M-treated HeLa cells (20 μ M \times 24 h). Representative images were captured under an inverted fluorescent microscope after DAPI staining. **(C)** Time dependent responses to I3M treatment. The percentage of sub-G1 events in HeLa, HepG2 and HCT 116 cells treated with 20 μ M I3M for the indicated time periods. Inserted are typical histograms derived from flow cytometry analysis of DNA content in control and I3M-treated HeLa cells (20 μ M \times 24 h). **(D)** Dose-dependent responses to I3M treatment. The percentage of sub-G1 events (upper panel) and MTT reduction (lower panel) in HeLa, HepG2 and HCT 116 cells were determined when treated with different concentrations of I3M for 24 h. **(E)** I3M-induced PARP cleavage in HeLa cells determined by western blot. Data in panel C and D are presented as means \pm S.D. from at least three independent experiments.

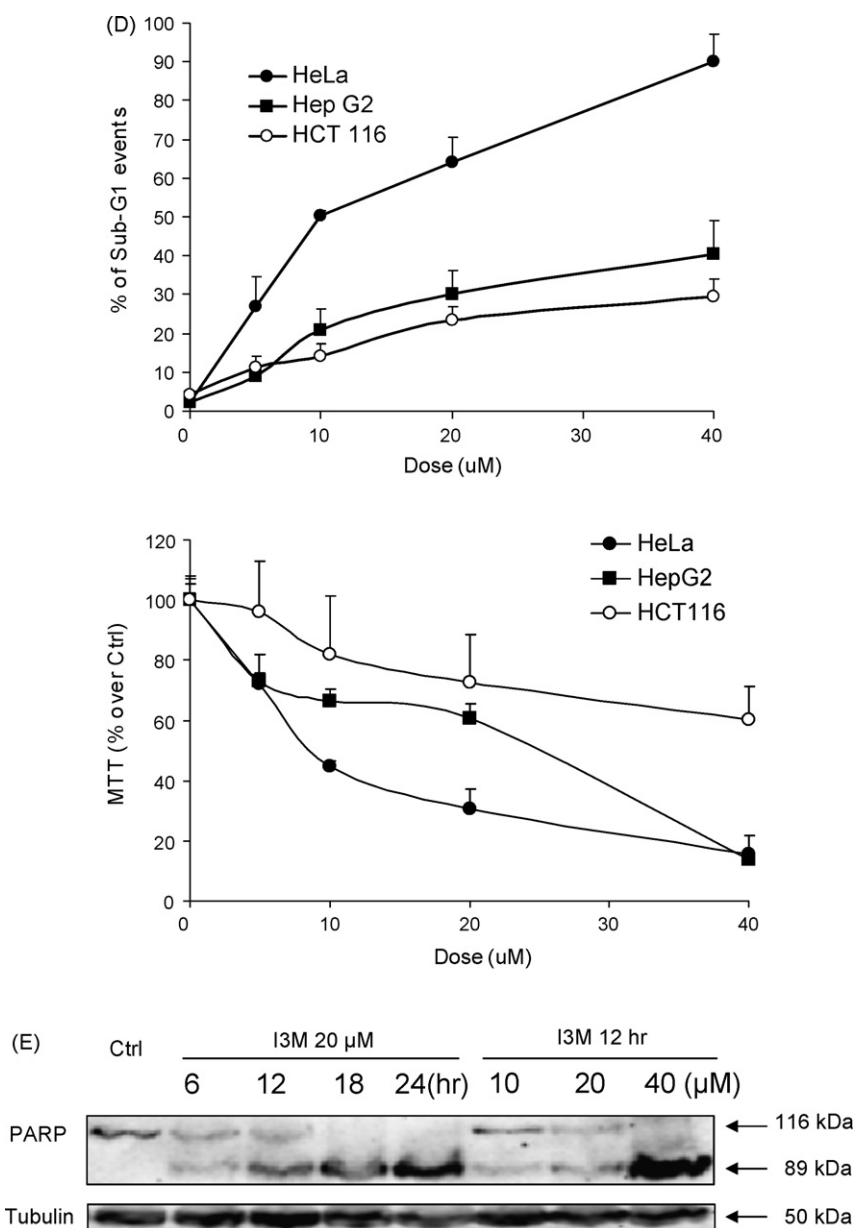


Fig. 1. (Continued).

Apoptosis or programmed cell death, plays a crucial role in the homeostasis of organisms under both physiological and pathological conditions; and targeting the malignant cells for apoptosis has always been an aim that various anti-cancer therapies tried to achieve [14,15]. It has been well established that the apoptotic stimuli transmit the death signals through the extrinsic (death receptor) and/or intrinsic (mitochondria) pathway [15]. The tumor suppressor gene p53 has been known to play a critical role in human tumorigenesis as a strong pro-apoptotic mechanism. Extensive studies have revealed p53-dependent transcriptional regulation of many pro-apoptotic genes involving both extrinsic and intrinsic pathways including DR5, Bax and Noxa [16]. In addition, Bcl-2 family proteins are also important regulators of apoptosis; according to the structural and functional characteristics, they are categorized

as anti-apoptotic members (such as Bcl-2 and Bcl-xL), multi-domain pro-apoptotic members (such as Bax and Bak) and BH3-only pro-apoptotic members (such as Bid and Bad) [17,18]. Type I cells undergo apoptosis only when caspase-8 directly activates the executioner caspase-3, whereas in type II cells, activated caspase-8 transmits the apoptotic signal to the mitochondria through Bcl-2 family members [19].

At present, the apoptotic pathway underlying indirubin and its derivatives-induced apoptotic cell death in cancer cells has not been fully elucidated. In this study, we investigated the involvement of the Bcl-2 family members in I3M-induced apoptotic machinery in human cervical cancer cell HeLa and our data demonstrate that I3M engages the extrinsic apoptotic pathway with a type II response, a process mediated by the pro-apoptotic Bcl-2 proteins, especially Bid and Bax.

2. Materials and methods

2.1. Chemicals and reagents

Iridubin-3'-monoxime (I3M), 4',6-diamidino-2-phenylindole (DAPI), and thiazolyl blue tetrazolium bromide (MTT), were purchased from Sigma–Aldrich Co. (St. Louis, MO, USA). Propidium iodide (PI) was purchased from Invitrogen-Molecular Probe (Eugene, OR, USA). Protease inhibitor cocktail was obtained from Roche Applied Science (Mannheim, Germany). Pan caspase inhibitor z-VAD-FMK, caspase-3 inhibitor ac-DEVD-CHO, caspase-8 inhibitor ac-IETD-CHO and caspase-9 inhibitor ac-LEHD-CHO were purchased from Biomol (Plymouth meeting, PA, USA); Another caspase-3 inhibitor z-DEVD-FMK was from Calbiochem (San Diego, CA, USA). Other common chemicals were from Sigma–Aldrich Co. Anti-PARP, anti-caspase-8, anti-bid, anti-caspase-9 (human specific), anti-caspase-3, and anti-COX IV antibodies were purchased from Cell Signaling Technology, Inc. (Beverly, MA, USA), anti-Bax (N-20) polyclonal, anti-DR4, anti-p53 (FL-393), and anti-p21 (C-19) antibody and goat anti-rabbit IgG HRP from Santa Cruz Biotechnology, Inc. (Santa Cruz, CA, USA), anti-DR5 antibody from Chemicon International, Inc. (Temecula, CA, USA), anti-cytochrome c monoclonal antibody from BD Biosciences Pharmingen (San Diego, CA, USA), anti- α -tubulin monoclonal antibody from Sigma, and ImmunoPure[®] peroxidase conjugated goat anti-mouse IgG (H + L) from Pierce Biotechnology (Rockford, IL, USA).

2.2. Cell culture and treatment

Human cervical cancer cell line HeLa, human hepatoma cell line HepG2 and human colorectal cancer cell line HCT116 were obtained from ATCC and maintained in Dulbecco's modified Eagle's medium (DMEM) (Sigma–Aldrich Co.) supplemented with 10% fetal bovine serum (FBS) (Hyclone, Logan, UT, USA) and antibiotics (Invitrogen, Carlsbad, CA, USA). Treatment details with I3M were illustrated in figure legends. All the chemical inhibitors were incubated 30 min before treatment.

2.3. Measurement of growth inhibition

MTT reduction has been frequently used for indicating growth inhibition [20]. Human cancer cells were seeded into 96-well plate 18 h prior to various treatments; each treatment group was seeded in triplicate; a group of empty wells were used as blank control. At the end of the treatment, medium in each well was removed, and 25 μ l of MTT (5 mg/ml in sterilized PBS) was added. After 1 h incubation at 37 °C with protection from light, 100 μ l lysis buffer (50% DMF and 15% SDS in dd-H₂O, pH 4.6–4.7) was added into each well; the plates were shaken on an orbital shaker till all the crystal formed dissolved completely. The absorbance reading was recorded by a microplate reader Tecan SpectraFluor Plus (MTX Lab Systems, Inc., Durham, NC, USA) at 590 nm.

2.4. Detection of apoptosis

Human cancer cells were treated by I3M and then the apoptosis were detected using the following methods: (i)

Morphological changes were observed under light microscope; and chromosomal condensation was detected by DAPI staining as previously described [21,22]. (ii) Percentage of the cells with hypodiploid DNA content was represented as percentage of sub-G1 events and measured by FACSCalibur (BD Biosciences, Heidelberg, Germany) using propidium iodide staining [23,24]. (iii) PARP cleavage was detected in whole-cell lysate by western blotting.

2.5. Caspase-3/7 activity assay

Caspase-3/7 activity was examined by Apo-One[®] Homogeneous Caspase-3/7 Assay (Promega Corporation, Madison, WI, USA) following manufacturer's instruction. After 1.5 h incubation, the fluorescence intensity was measured at 535 nm using Tecan SpectraFluor Plus.

2.6. Measurement of surface expression of death receptors

Not more than one million HeLa cells, untreated or treated with I3M (20 μ M \times 24 h), were stained with Phycoerythrin (PE)-labeled DR4 or DR5 (eBioscience, Inc., San Diego, CA, USA) at room temperature for 30 min at dark. To control for nonspecific binding, PE-conjugated mouse IgG1, K isotype control were used as isotype-matched nonbinding antibodies. 20 μ l of each of the specific antibodies or the isotype antibody together with 30 μ l staining buffer was used for each sample. Cells were washed once with staining buffer before analysis by FACSCalibur using Cellquest software (BD Biosciences).

2.7. Detection of Bax conformational changes by immunoprecipitation and immunofluorescence

Immunoprecipitation was carried out as previously described [21] with minor changes. Briefly, cells were lysed in CHAPS lysis buffer (10 mM Hepes, pH 7.4, 150 mM NaCl, 1% CHAPS) containing protease inhibitors [4]. The cell lysates were normalized for protein content and pre-cleared by incubating 500 μ g of total protein with 50 μ l of protein G-agarose for 60 min on ice. After spinning at 10,000 \times g for 10 min, pre-cleared lysate (supernatant) were transferred to a new eppendorf tube and incubated with 2 μ g of anti-Bax 6A7 monoclonal antibody (Sigma–Aldrich Co.) in 500 μ l of CHAPS lysis buffer overnight at 4 °C. Afterwards, 25 μ l of protein G-agarose were added and incubated for additional 3 h at 4 °C. Protein G-agarose beads were washed carefully in CHAPS lysis buffer for 3 times and then boiled in loading buffer containing 5% β -mercaptoethanol. Conformational changed Bax in the immunoprecipitates were detected by western blot using anti-Bax polyclonal antibody. For immunofluorescence, HeLa cells were seeded in 8-well chamber slides (NALGENE[®] NUNC[™], Rochester, NY, USA) 24 h before treatment. After treatment cells were fixed in 3% paraformaldehyde for 30 min at room temperature and permeabilized for 2 min with 0.2% CHAPS in PBS. After blocking with PBS containing 0.2% Tween-20, 5% FBS and 3% BSA for 1 h, cells were incubated with anti-Bax 6A7 antibody overnight at 4 °C. After washing with PBS containing 0.2% Tween-20, cells were incubated with anti-mouse Alexa 633 secondary antibody for another 1 h at room temperature. Coverslips were mounted onto slides using ProLong anti-fade mounting

reagent (Invitrogen-Molecular Probe). Cells were then visualized under Olympus FLOVIEW V500 confocal microscope with 60× oil lens.

2.8. Western blot

Western blot analysis was performed as previously described [21]. Whole-cell lysate was prepared by lysing cells in M2 buffer (20 mM Tris, pH 7.4, 0.5% NP-40, 250 mM NaCl, 3 mM EDTA, 3 mM EGTA, 2 mM dithiothreitol (DTT), 0.5 mM phenylmethylsulfonyl fluoride (PMSF), 20 mM β -glycerol phosphate, 1 mM sodium vanadate and 1× protease inhibitor cocktail) and insoluble fractions were discarded after centrifugation at 15,000 g for 18 min. Equal amount of proteins were fractionated on SDS-PAGE gel in the Mini-PROTEAN II system (Bio-Rad Laboratories, Hercules, CA, USA) and blotted onto PVDF membrane (Millipore Corporation, Billerica, MA, USA). After blocking with 5% nonfat milk in TBST (10 mM Tris-HCl, 100 mM NaCl and 0.1% Tween-20), the membrane was probed with various primary antibodies followed by corresponding secondary antibodies, and then developed with enhanced chemiluminescence (Pierce Biotechnology) using a Kodak Image Station 440CF (Kodak, Rochester, NY, USA). α -Tubulin was used as loading control.

2.9. Transient transfection

HeLa cells were seeded 12 h before transfection in antibiotics-free medium and 90% confluency was achieved at the point of transfection. Cells were transfected with pcDNA3.1 empty vector, Bcl-2 expression vector or CrmA expression vector (a

kind gift from Dr. ZG Liu, NCI, USA) using Lipofectamine™ 2000 (Invitrogen) according to the manufacturer's instructions; PmaxGFP vector (Amara Inc., Gaithersburg, MD, USA) was co-transfected as a transfection marker and only successful transfected cells were analyzed as described before [25]. Briefly speaking, only cells expressing green fluorescent protein (GFP), as detected by FACSCalibur, were analyzed for their DNA content and presented in the data. The voltage used was determined by control samples with or without GFP expression. After 48 h of transfection, the cells were treated with 20 μ M I3M for 24 h. Cell death was determined by percentage of sub-G1 events and morphological changes examined under inverted fluorescent microscope (Nikon Corporation, Tokyo, Japan).

2.10. Establishment of stable cell line with siRNA knockdown

HeLa cells with stable knockdown of Bid, was generated using pSuper vector containing the following sequence: forward strand 5'-GATCCCC CCATAGAGGATGGTCTTAC TTCAAGAGA GTAAGACCATCCTCTATGG TTTTGGAAA-3'; reverse strand 5'-AGCTTTTCCAAAAA CGATAGAGGATGGTCTTAC TCTC-TTGAA TAACCATTTCGTGGGTGGTC GGG-3', which carries a neomycin selection marker (a gift from Dr. ZW Song, BTI, Singapore). Corresponding control HeLa cells expressing empty pSuper vector with neomycin selection marker were also generated. After transient transfection of the above pSuper vectors, cells that survived 2 weeks of selection were used to generate single cell clones by limiting dilution. G418 Sulfate (Promega Biotechnology) 500 μ g/ml was applied in the

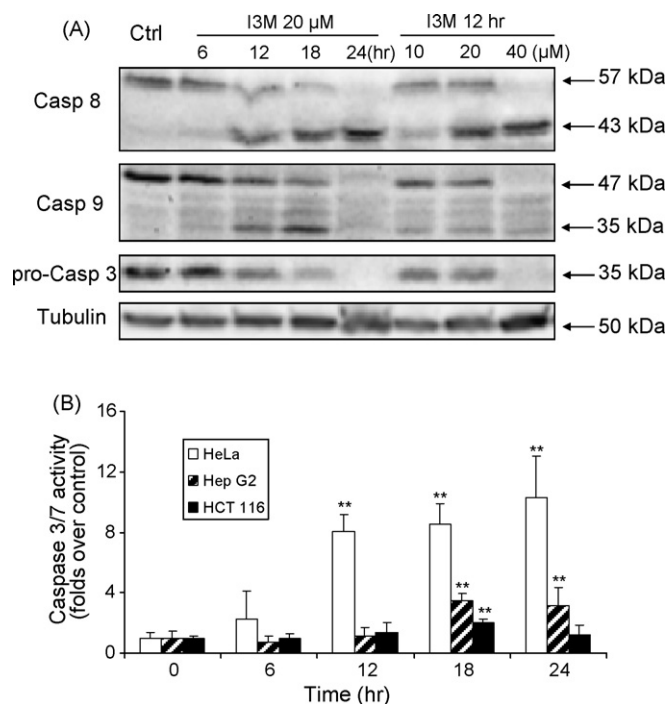


Fig. 2 – I3M-induced caspase activation. (A) I3M-induced caspase-8, -9 and -3 cleavages in HeLa cells determined by western blot. **(B)** I3M-induced caspase-3/7 activity measured by Apo-One™ Caspase-3/-7 Assay Kit. Three types of cancer cells were treated by 20 μ M I3M for the indicated time periods. Data are presented as means \pm S.D. from at least three independent experiments.

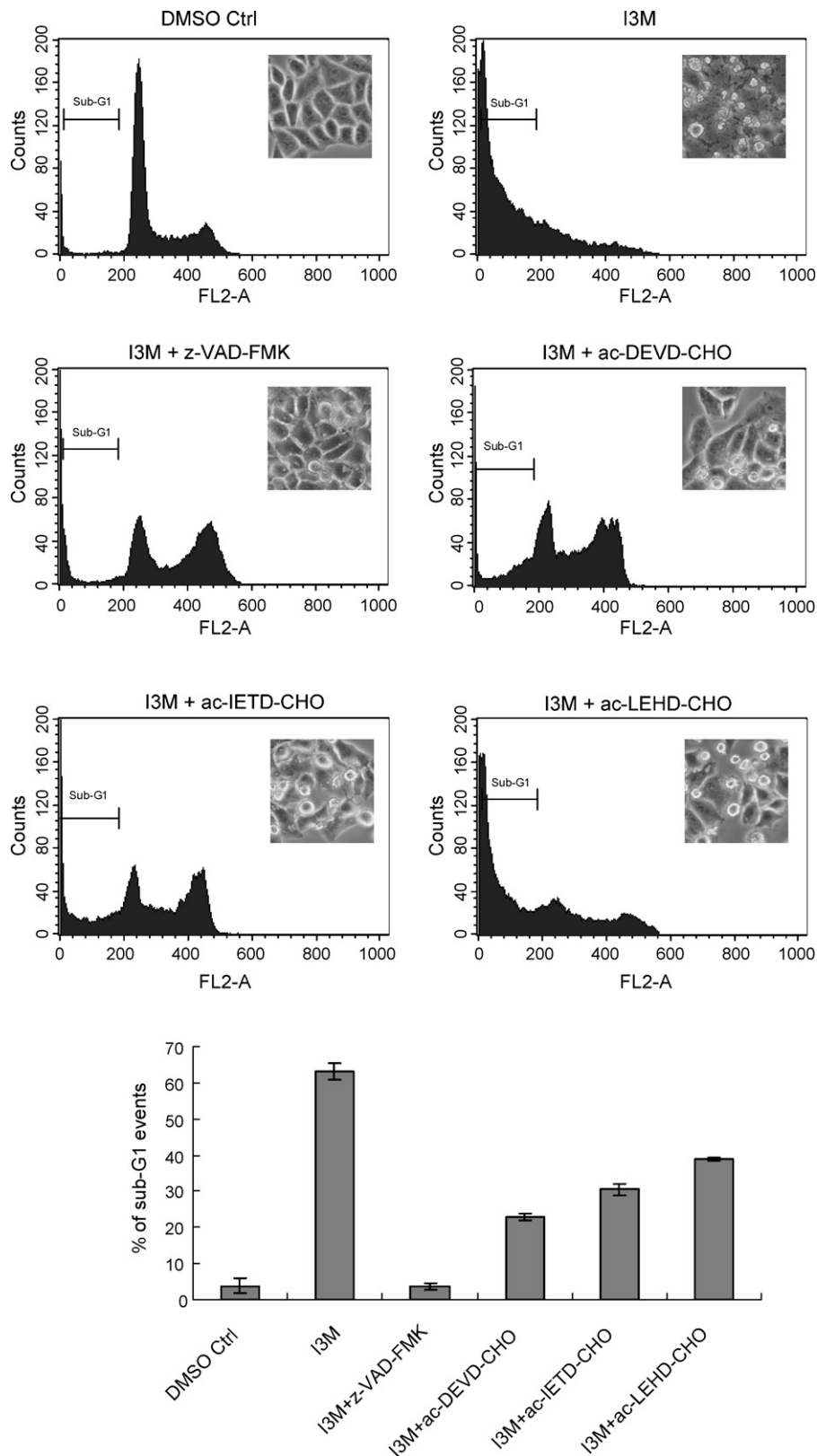


Fig. 3 – Inhibition of I3M-induced apoptosis by synthetic caspase inhibitors. HeLa cells were treated by 20 μ M I3M together with individual caspase inhibitor for 24 h at the following concentration: 50 μ M z-VAD-FMK, 200 μ M ac-DEVD-CHO, 200 μ M ac-IETD-CHO, or 200 μ M ac-LEHD-CHO. Each treatment is represented by a typical histogram showing the sub-G1 peak and an inserted image showing HeLa cell morphology under light microscopy (upper panel). The bar chart (lower panel) summarizes the percentage of sub-G1 events under different treatment condition. Data are presented as means \pm S.D. from at least three independent experiments.

complete DMEM medium during selection and after selection, but not during any treatment.

2.11. Statistics

All numerical data were presented as mean \pm S.D. of at least three independent experiments. Statistical significance was assessed by Student's *t*-tests. *P* values less than 0.05 were considered significant.

3. Results

3.1. I3M induces apoptosis in a time- and dose-dependent manner in human cancer cells

With I3M treatment, we observed the characteristics of apoptosis—membrane blebbing, chromosomal condensation

and DNA fragmentation in HeLa (Fig. 1B), as well as in HepG2 and HCT116 (data not shown). I3M-induced apoptosis was quantified using sub-G1 analysis and MTT assay; we observed a time- and dose-dependent manner in the three cancer cells (Fig. 1C and D). Among them, HeLa cells are most susceptible to I3M. In addition, PARP cleavage, another hallmark of apoptosis, was also detected in HeLa cells in a similar time and dose-dependent pattern (Fig. 1E). Similar results were observed in HepG2 and HCT116 cells (data not shown).

3.2. I3M induces caspase activation

To understand the apoptotic machinery involved in I3M-induced apoptosis, we examined caspase activation. Evident caspase-8 cleavage commenced at 12 h and almost all were cleaved at 24 h (Fig. 2A). Cleavage of caspase-9 and -3 was also detected in a similar temporal pattern (Fig. 2A). In addition, we quantified the activity of effector caspases (caspase-3/7) in the

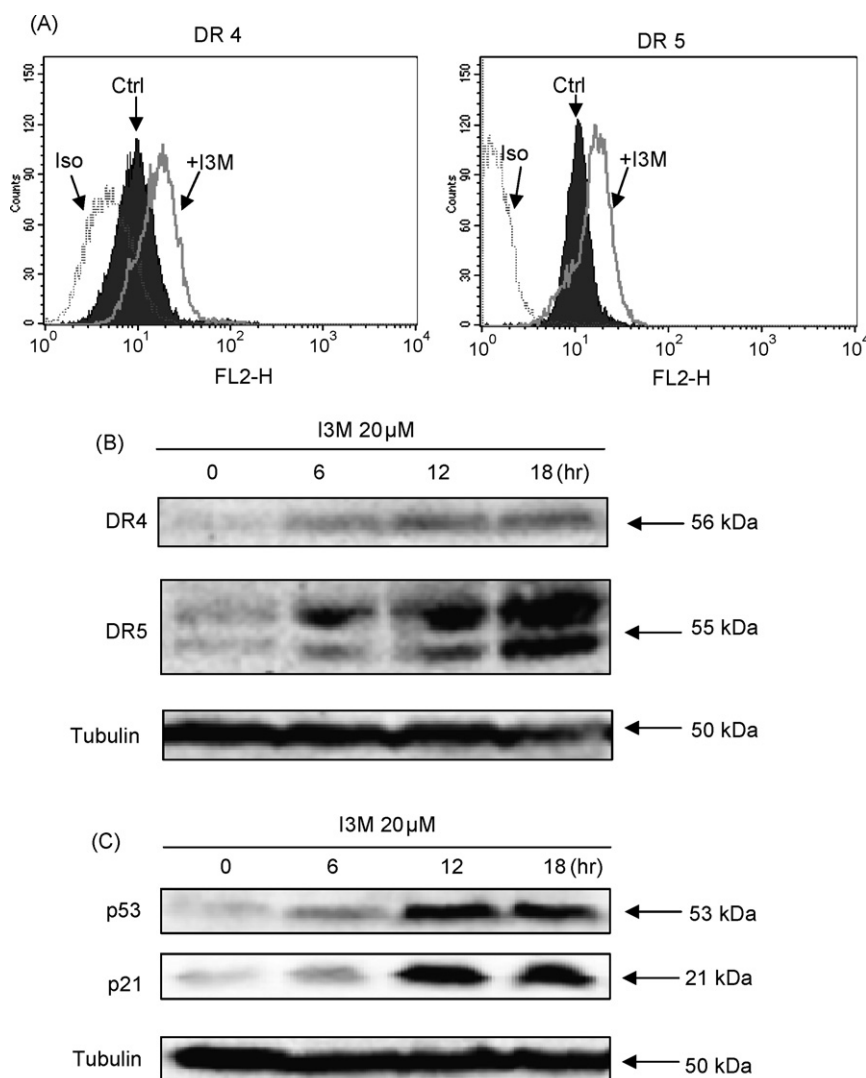


Fig. 4 – I3M-induced enhanced surface expression of DR4 and DR5. (A) Surface expression of DR4 and DR5. Untreated HeLa cells (Ctrl) and HeLa cells upon 9 h of exposure to I3M (20 μ M) were analyzed by FACS using PE-conjugated DR4 and DR5 antibodies. Isotype-matched antibodies (Iso) were used to control for unspecific binding. **(B)** Total protein level for DR4 and DR5 determined by western blot. The cells were treated with I3M as indicated. **(C)** I3M-induced p53 and p21 up-regulation. HeLa cells were treated as indicated and protein levels were determined by western blot.

three cancer cells and found that the degree of activity corresponded to that of apoptosis detected by sub-G1 analysis (Figs. 1C and 2B).

To confirm the involvement of the above-mentioned caspases, we utilized various synthetic caspase inhibitors to test their protective effects on I3M-induced cell death. Pretreatment with a pan-caspase inhibitor (z-VAD-FMK) completely protected I3M-induced apoptosis (Fig. 3). In contrast, pretreatment with a caspase-3 inhibitor (ac-DEVD-CHO), a caspase-8 inhibitor (ac-IETD-CHO) or a caspase-9 inhibitor (ac-LEHD-CHO) only partially protected apoptosis induced by I3M (Fig. 3). Data from Figs. 2 and 3 collectively suggest that caspases involved in both the extrinsic and intrinsic pathways are activated in I3M-induced apoptosis.

3.3. I3M induces increased surface expression of death receptors accompanying p53 up-regulation

To provide a possible mechanism for the activation of the extrinsic pathway induced by I3M, we first evaluated the surface expression of the death receptor 4 and 5 (DR4 and DR5) in HeLa cells. Upon treatment with I3M for 9 h, levels of both receptors increased significantly (Fig. 4A). Such observations were confirmed by the total protein level of DR4 and DR5 determined by western blot (Fig. 4B). It has been reported that the expression of DR4 and DR5 is transcriptionally regulated by tumor suppressor gene p53 [26,27]. Here we also observed a time-dependent increase (with a peak at 12 h) of p53 protein level in cells treated with I3M (Fig. 4C). The concurrent increase of p21 protein level indicated the transcriptional activation of p53 induced by I3M in HeLa cells (Fig. 4C).

3.4. I3M induces Bid cleavage

The extrinsic death receptor pathway can initiate the mitochondrial amplification loop in type II cells by caspase-8 mediated Bid cleavage and subsequent translocation of tBid

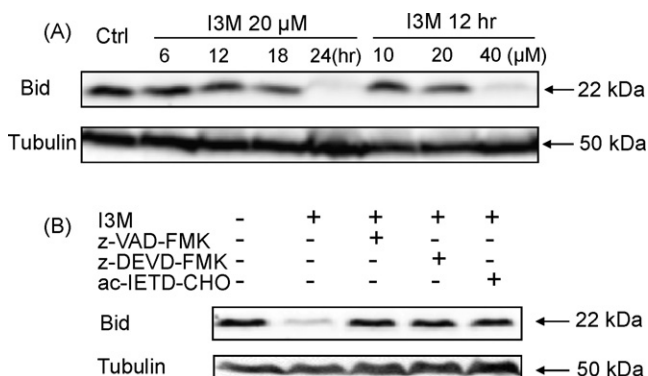


Fig. 5 – Bid cleavage in response to caspase activation in I3M-induced apoptosis. (A) I3M-induced Bid cleavage in a time- and dose-dependent manner in HeLa cells under the indicated treatment conditions. **(B)** Caspase inhibitors blocked I3M-induced Bid cleavage. HeLa cells were treated with 20 μM I3M for 24 h with the absence or presence of 50 μM individual caspase inhibitor.

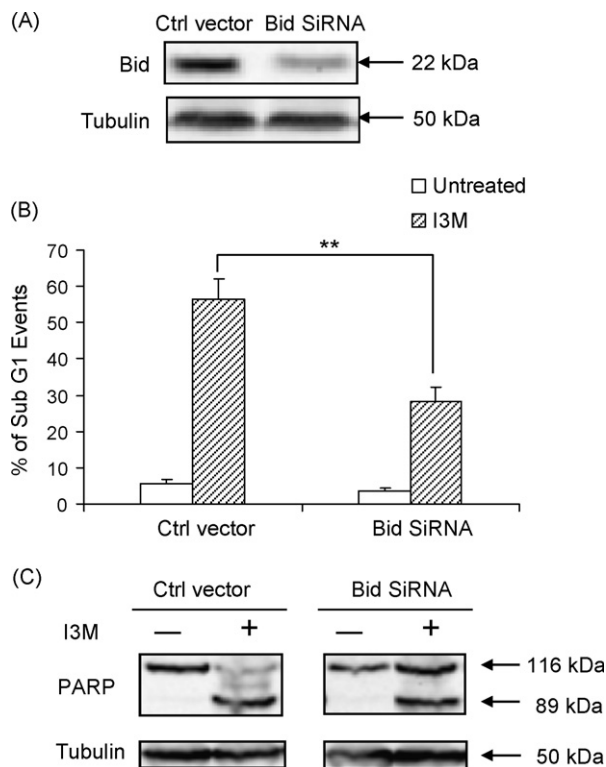


Fig. 6 – Protection conveyed by Bid knockdown against I3M-induced apoptosis. (A) Reduction of Bid protein level in HeLa cells with stable expression of the pSuper Bid SiRNA vector in comparison to cells with the control vector. **(B)** Protection against I3M-induced apoptosis in HeLa cells stably expressing Bid SiRNA. Cells were treated with I3M (20 μM × 24 h) and apoptosis was measured by percentage of sub-G1 events. Data are presented as means ± S.D. from three independent experiments. Statistical significance was analyzed by Student's t-test ($p < 0.01$ when compared with the control group; the degree of freedom is 1). **(C)** Bid knockdown partially protected I3M-induced PARP cleavage. HeLa cells stably expressing either the control vector or Bid SiRNA were treated with I3M (20 μM × 24 h). PARP cleavage was determined as Fig. 1E.

to the mitochondria [28,29]. In this study, since I3M-induced apoptosis involves both caspase-8 and -9 activation (Fig. 2A), we thus examined whether I3M could induce Bid cleavage. I3M led to evident Bid cleavage (Fig. 5A) which was completely prevented by a pan-caspase inhibitor (z-VAD) or a caspase-8 inhibitor (Ac-IETD) (Fig. 5B), in correspondence with the pattern of protection regarding cell death (Fig. 3). In order to confirm the role of Bid in I3M-induced apoptosis, we established the stable Bid knockdown HeLa cells using the siRNA technique (Fig. 6A). In HeLa cells with Bid stable knockdown, there is a 50% reduction for the percentage of apoptosis induced by I3M as determined by sub-G1 analysis (Fig. 6B). Consistently, PARP cleavage was also partially salvaged comparing to the cells expressing the control vector (Fig. 6C).

3.5. I3M induces Bax conformational changes

In response to Bid or other BH3-only proteins, multi-domain pro-apoptotic Bcl-2 family members, such as Bax and Bak, can be conformationally activated to form homo-multimers/complex in the mitochondrial membrane and thereby increase the membrane permeability [17]. Here we investigated the conformational change of Bax using the following two methods: (i) immunofluorescence detected using a specific antibody (anti-Bax 6A7) that can recognize the N-terminal of the transformed Bax [30,31], and (ii) immunoprecipitation and western blot. In I3M-treated HeLa cells, there is time- and dose-dependent increase of red fluorescence (Fig. 7A), indicating the increased amount of transformed Bax. Such results are consistent with the immunoprecipitation data in Fig. 7B that there is a time- and dose-dependent increase of Bax pulled down by anti-Bax 6A7. Bands at about 42 kDa were observed in Fig. 7B and suspected to be the dimmer form of Bax. Furthermore, Bax conformational change was caspase-dependent as both a pan-caspase inhibitor (z-VAD) and a caspase-8 inhibitor (ac-IETD) significantly blocked such changes (Fig. 7C). Finally, Bid knockdown also significantly suppressed Bax conformational changes induced by I3M (Fig. 7D), suggesting that Bax acts downstream of Bid in I3M-induced apoptosis.

3.6. Overexpression of Bcl-2 or CrmA partially blocks I3M-induced apoptosis

Data presented above highlight the critical role of the pro-apoptotic Bcl-2 family members in I3M-induced apoptosis at

the site of mitochondria. Here we used genetic approaches to further examine the role of the anti-apoptotic Bcl-2 protein in I3M-induced apoptosis. HeLa cells were transiently transfected with expression vector of either Bcl-2 protein or the viral protein cytokine response member A (CrmA), a known specific caspase-8 inhibitor [32], together with a green fluorescent protein construct as a transfection marker. The ectopically expressed Bcl-2 protein was also measured using western blot to confirm the successful transfection in HeLa cells (data not shown). For a more reliable analysis of the effects of overexpressed Bcl-2 or CrmA on I3M-induced apoptosis, we analyzed the DNA content/sub-G1 profile only among the transfected cell population (Fig. 8A). Based on the morphological changes (data not shown) and flow cytometry analysis of those transfected cells (Fig. 8B), overexpression of CrmA or Bcl-2 provided strong protection against I3M-induced cell death (Fig. 8C).

4. Discussion

Previous studies have demonstrated that indirubin and its derivatives are promising anti-cancer agents based on the following observations: (i) they are capable of selectively inducing apoptotic cell death in a wide spectrum of human cancer cells with minimal toxicity on normal cells [4–8]; and (ii) *in vivo* study in rat model has proved their efficacy in arresting tumor growth [8]. However, the molecular mechanisms underlying the apoptotic cell death induced by indirubin and its derivatives have not been fully elucidated. In this study

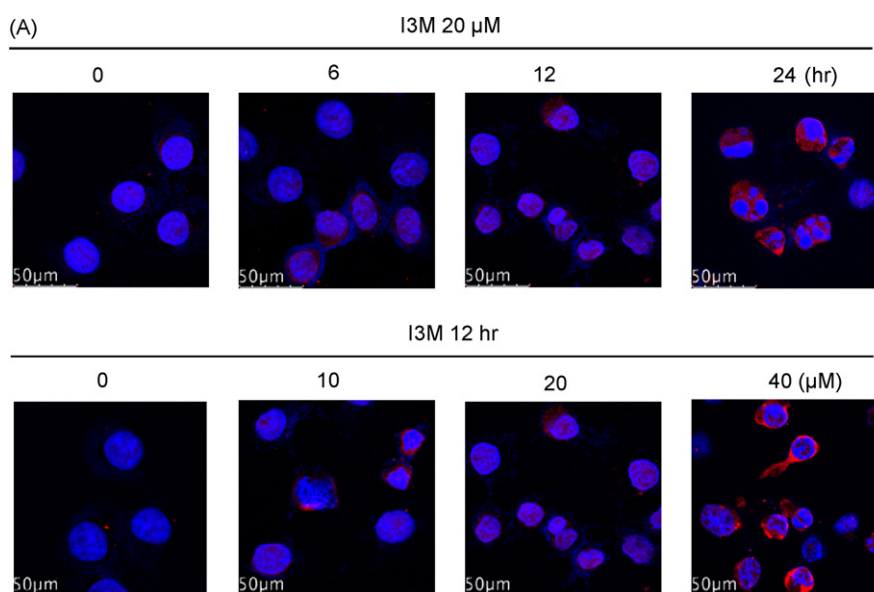


Fig. 7 – Bax conformational change following caspase-8 activation in I3M-treated HeLa cells. (A) Conformational changes of Bax detected by immunofluorescence staining and shown in red fluorescence. Cell nuclei were counterstained by DAPI. Representative images were captured using an inverted fluorescence microscope. (B) Conformational changes of Bax detected by immunoprecipitation (IP) and western blot (WB). Following designated treatments, transformed Bax was immunoprecipitated using anti-Bax 6A7 antibody and then subject to western blot analysis using anti-Bax N-20 antibody. (C) Caspase-dependent Bax conformational change. HeLa cells were treated with I3M (20 μM) with the presence of caspase inhibitors (50 μM) for 24 h and the transformed Bax was detected as in panel A. (D) Reduced Bax conformational change in HeLa cells stably expressing Bid siRNA. Cells were treated with 20 μM I3M for 24 h and the transformed Bax was detected as in panel A.

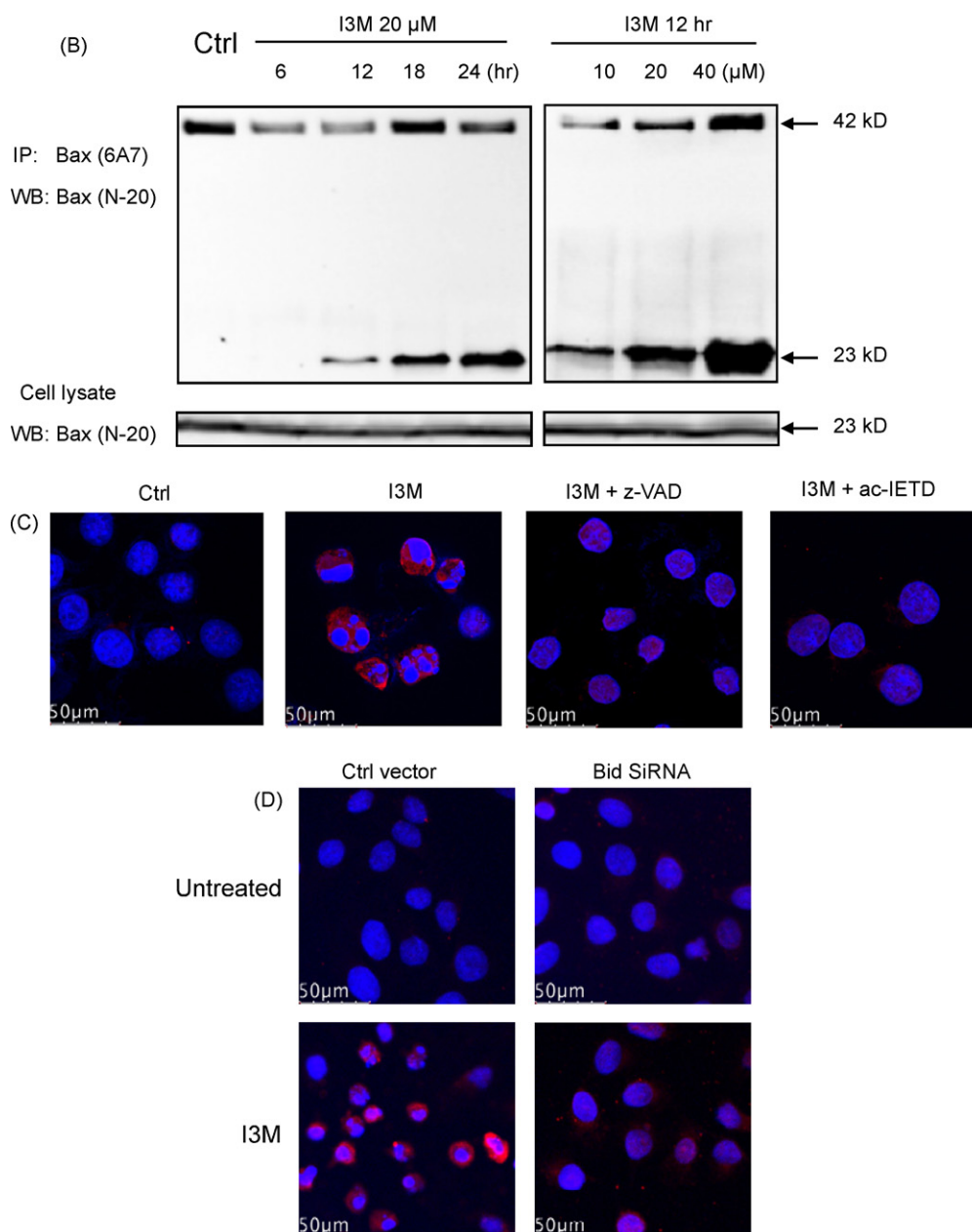


Fig. 7. (Continued).

we provide convincing evidence demonstrating that I3M-induced apoptosis engages the extrinsic death receptor pathway with a type II-cell behavior in which the pro-apoptotic bcl-2 family members Bid and Bax play a critical role.

Our study is the first to prove the involvement of the extrinsic death receptor pathway in I3M-induced apoptosis, as demonstrated by evident caspase-8 activation at early time points (Fig. 2A), and the protective effect of a synthetic caspase-8 inhibitor (Fig. 3), as well as overexpression of a viral caspase-8 inhibitor CrmA (Fig. 8B and C). Similar mechanism of action has been reported for a number of other natural products. For example, andrographolide, an extract from a traditional herbal medicine *Andrographis paniculata*, has been shown to induce apoptosis in HepG2 cells via caspase-8

activation [21]. Similarly, prodelphinidin B-2,3,3'-di-gallate from *Myrica rubra* [33] and the water extract of *Phyllanthus urinaria* have been shown to trigger apoptosis via the Fas/FasL system [34]. Furthermore, we observed increased surface expression, as well as total protein level, of both death receptor DR4 and DR5 in HeLa cells upon I3M treatment (Fig. 4A and B). DR4 and DR5, also known as TRAIL-R1 and TRAIL-R2, respectively, contain functional cytoplasmic death domain motifs, which associate with Fas-associated death domain protein (FADD) upon activation by apoptotic signals such as TRAIL [35,36]. FADD contains the death effector domain and is involved in the activation of caspase-8 [37]. Therefore, increased surface expression of DR4 and DR5 observed in I3M-treated cells (Fig. 4A) might contribute to the

caspase-8 activation observed in Fig. 2A. It has been reported that expression of DR4 or DR5 is transcriptionally regulated by p53 tumor suppressor gene [26,27]. In this study, the significantly elevated p53 and p21 protein level in I3M-treated cells (Fig. 4C) suggests the possibility that I3M promotes DR4 and DR5 expression via activation of p53. Although a number of previous studies have shown that HeLa cells are either p53 deficient [38] or with low expression level of p53 [39], it has also been reported that in HeLa cells p53 could be functionally up-regulated as evidenced by the increase of p21 protein [40]. In fact, treatment using other indirubin derivatives have been observed to up-regulate p53 in human cancer cells [4,6], implying a common mechanism in indirubin derivative-induced apoptosis. At present, it remains to be further tested as how I3M induces p53 accumulation and activation.

Another possible mechanism by which I3M promotes death receptor-mediated apoptosis is through modulation of NF- κ B activity. The anti-apoptotic function of NF- κ B has been well established via the transcriptional regulation of various anti-apoptotic genes such as (c-FLIP, cIAP1/2, and Survivin) [41,42]. Indirubin and its derivatives have been reported to inhibit the NF- κ B signaling pathway stimulated by various activators, including TNF α , PMA and H₂O₂ [12]. In this study, I3M did not affect the basal level of NF- κ B transcriptional activity (data not shown). It remains to be further studied

whether I3M-mediated caspase-8 activation is achieved via the suppression of the NF- κ B signaling pathway.

On the other hand, I3M-induced apoptosis in HeLa cells also exhibit a response typical of type II cells, since the intrinsic mitochondrial pathway as demonstrated by caspase-9 activation (Fig. 2A) and cytochrome c release (data not shown) is mediated by Bid cleavage (Fig. 5A) downstream of caspase-8 activation (Fig. 5B). Furthermore, Bax conformational change occurs as the consequences of caspase-8 activation (Fig. 7C) and Bid cleavage (Fig. 7D) based on immunofluorescence (Fig. 7A) and immunoprecipitation (Fig. 7B) data using conformation-specific antibody 6A7. In addition to BH3-only proteins, the anti-apoptotic Bcl-2 family members are also known to modulate the pro-apoptotic activity of Bax through sequestering Bax by the formation of heterodimers [43]. In the present study, ectopic expression of Bcl-2 protein offered moderate protection against I3M-induced cell death (Fig. 8B and C). Collectively the above evidence suggests that I3M-induced apoptosis in HeLa cells displays a type II cell response with the engagement of both the anti-apoptotic and pro-apoptotic Bcl-2 family members at the site of mitochondria.

In summary, data from this study reveal the apoptotic mechanism of I3M in human cervical cancer cell HeLa: extrinsic death receptor pathway accompanied by type II

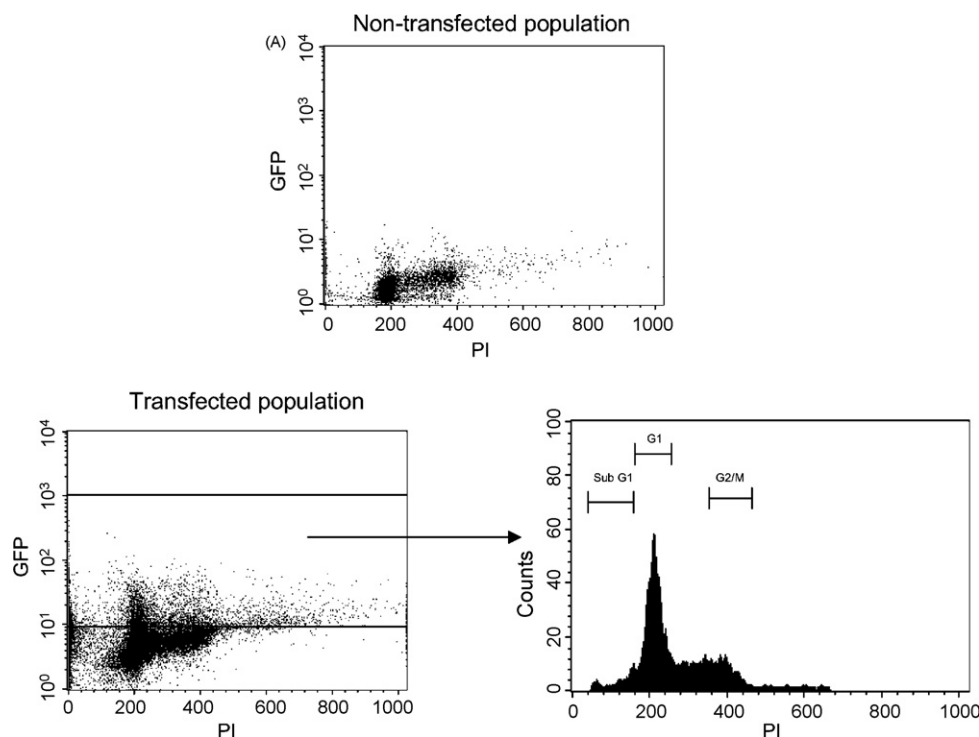


Fig. 8 – Ectopic expression of Bcl-2 or CrmA protects against I3M-induced apoptosis. (A) HeLa cells were first transiently transfected with pcDNA empty vector, Bcl-2, or CrmA expression vector, respectively, together with PmaxGFP as a transfection marker. 48 h post transfection, cells were treated with I3M (20 μ M \times 24 h) and then collected and stained with PI for DNA content analysis. Among total of 20,000 cells from each group analyzed using flow cytometry, only those transfected cells with GFP expression and PI staining were presented for the analysis of sub-G1 events. (B) Representative histograms from each transfection group with or without I3M treatment. (C) Quantification of percentage of sub-G1 events. Data are presented as means \pm S.D. from three independent experiments. Statistical significance was analyzed by Student's t-test ($^*p < 0.01$ when compared with the pcDNA group; $^*p < 0.05$; the degree of freedom is 1).

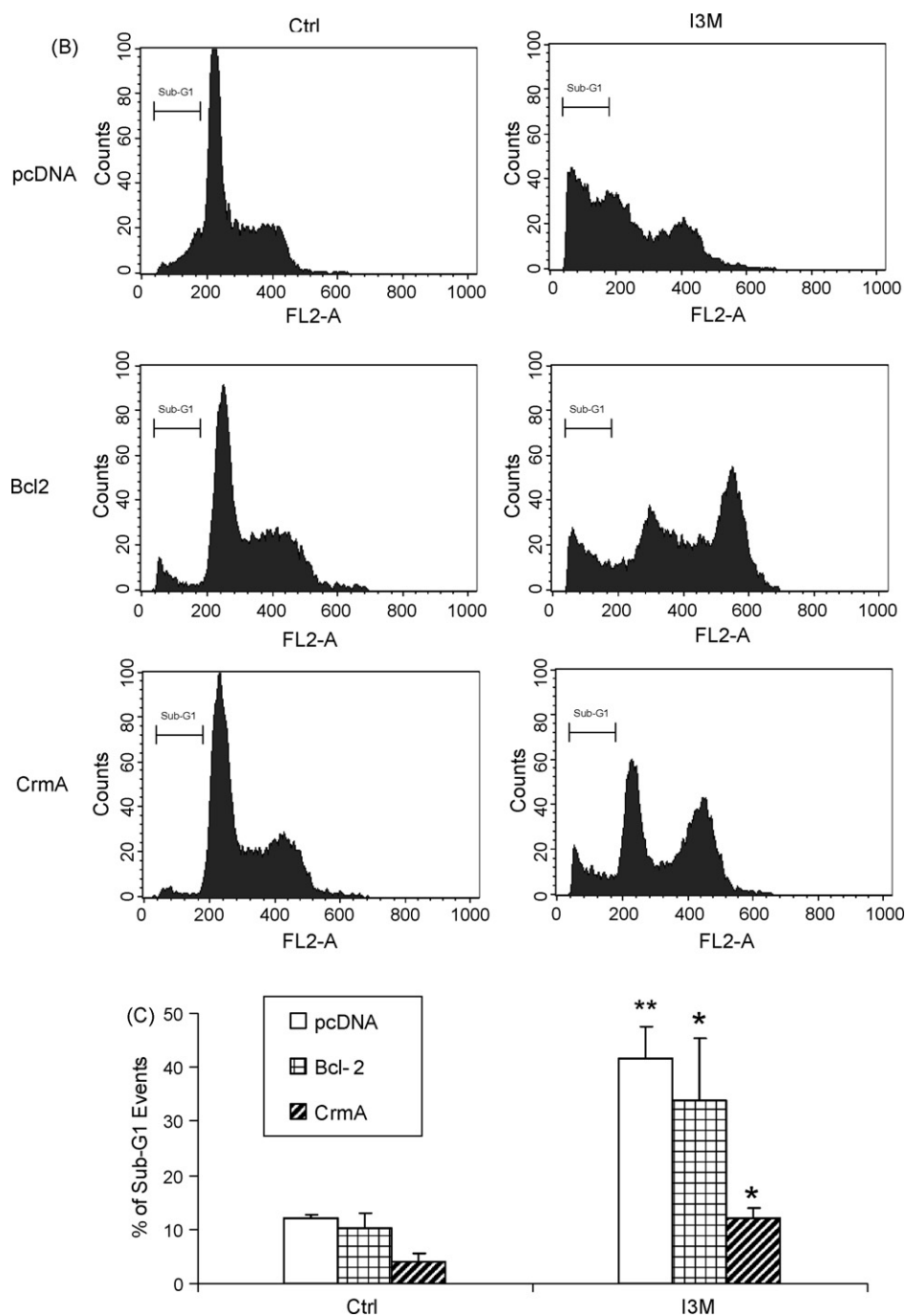


Fig. 8. (Continued).

response with critical involvement of the pro-apoptotic Bcl-2 family members (Bid and Bax). Indirubin and its derivatives have been known for their potential anti-tumor activities. Therefore understanding of such mechanisms provides the basis for future studies to expand the scope of their anti-cancer effects. For instance, indirubins have been reported to sensitize TNF α -induced and Taxol-induced apoptosis [12]. Based on the observation of our study that I3M promotes the DR4 and DR5 expression, the sensitization effect of I3M on TRAIL-induced apoptosis especially in those TRAIL-resistant

cancer cells would be highly promising and provides a direction for future studies.

Acknowledgements

This study was supported by research grants from the National Medical Research Council (NMRC), Biomedical Research Council (BMRC) and Academic Research Fund (ARF). J. Shi is a Research scholar supported by the National

University of Singapore. We thank Dr. Song Z.W. for providing the Bid siRNA expression vector, Mr. Ong Y.B. and Ms. Zhao M. for their technical support.

REFERENCES

- [1] Xiao Z, Hao Y, Liu B, Qian L. Indirubin and meisoindirubin in the treatment of chronic myelogenous leukemia in China. *Leuk Lymphoma* 2002;43:1763–8.
- [2] Eisenbrand G, Hippe F, Jakobs S, Muehlbeyer S. Molecular mechanisms of indirubin and its derivatives: novel anticancer molecules with their origin in traditional Chinese phytochemistry. *J Cancer Res Clin Oncol* 2004;130:627–35.
- [3] Hoessel R, Leclerc S, Endicott JA, Nobel ME, Lawrie A, Tunnah P, et al. Indirubin, the active constituent of a Chinese antileukaemia medicine, inhibits cyclin-dependent kinases. *Nat Cell Biol* 1999;1:60–7.
- [4] Yamaguchi H, Paranawithana SR, Lee MW, Huang Z, Bhalla KN, Wang HG. Epothilone B analogue (BMS-247550)-mediated cytotoxicity through induction of Bax conformational change in human breast cancer cells. *Cancer Res* 2002;62:466–71.
- [5] Nam S, Buettner R, Turkson J, Kim D, Cheng JQ, Muehlbeyer S, et al. Indirubin derivatives inhibit Stat3 signaling and induce apoptosis in human cancer cells. *Proc Natl Acad Sci USA* 2005;102:5998–6003.
- [6] Ribas J, Bettayeb K, Ferandin Y, Knockaert M, Garrofe-Ochoa X, Totzke F, et al. 7-Bromoindirubin-3'-oxime induces caspase-independent cell death. *Oncogene* 2006;25:6304–18.
- [7] Perabo FG, Frossler C, Landwehrs G, Schmidt DH, von Rucker A, Wirger A, et al. Indirubin-3'-monoxime, a CDK inhibitor induces growth inhibition and apoptosis-independent up-regulation of surviving in transitional cell cancer. *Anticancer Res* 2006;26:2129–35.
- [8] Kim SA, Kim YC, Kim SW, Lee SH, Min JJ, Ahn SG, et al. Antitumor activity of novel indirubin derivatives in rat tumor model. *Clin Cancer Res* 2007;13:253–9.
- [9] Leclerc S, Garnier M, Hoessel R, Marko D, Bibb JA, Snyder GL, et al. Indirubins inhibit glycogen synthase kinase-3 beta and CDK5/p25, two protein kinases involved in abnormal tau phosphorylation in Alzheimer's disease. A property common to most cyclin-dependent kinase inhibitors? *J Biol Chem* 2001;276:251–60.
- [10] Meijer L, Skaltsounis AL, Magiatis P, Polychronopoulos P, Knockaert M, Leost M, et al. GSK-3-selective inhibitors derived from Tyrian purple indirubins. *Chem Biol* 2003;10:1255–66.
- [11] Adachi J, Mori Y, Matsui S, Takigami H, Fujino J, Kitagawa H, et al. Indirubin and indigo are potent aryl hydrocarbon receptor ligands present in human urine. *J Biol Chem* 2001;276:31475–8.
- [12] Sethi G, Ahn KS, Sandur SK, Lin X, Chaturvedi MM, Aggarwal BB. Indirubin enhances tumor necrosis factor-induced apoptosis through modulation of nuclear factor-kappa B signaling pathway. *J Biol Chem* 2006;281:23425–3.
- [13] Zhen Y, Sorensen V, Jin Y, Suo Z, Wiedlocha A. Indirubin-3'-monoxime inhibits autophosphorylation of FGFR1 and stimulates ERK1/2 activity via p38 MAPK. *Oncogene* 2007.
- [14] Fesik SW. Promoting apoptosis as a strategy for cancer drug discovery. *Nat Rev Cancer* 2005;5:876–85.
- [15] Fulda S, Debatin KM. Extrinsic versus intrinsic apoptosis pathways in anticancer chemotherapy. *Oncogene* 2006;25:4798–811.
- [16] Haupt S, Berger M, Goldberg Z, Haupt Y. Apoptosis—the p53 network. *J Cell Sci* 2003;116:4077–85.
- [17] Tsujimoto Y. Cell death regulation by the Bcl-2 protein family in the mitochondria. *J Cell Physiol* 2003;195:158–67.
- [18] Cory S, Adams JM. The Bcl2 family: regulators of the cellular life-or-death switch. *Nat Rev Cancer* 2002;2:647–56.
- [19] Boehrer S, Nowak D, Hoelzer D, Mitrou PS, Chow KU. The molecular biology of TRAIL-mediated signaling and its potential therapeutic exploitation in hematopoietic malignancies. *Curr Med Chem* 2006;13:2091–100.
- [20] Hansen MB, Nielsen SE, Berg K. Re-examination and further development of a precise and rapid dye method for measuring cell growth/cell kill. *J Immunol Methods* 1989;119:203–10.
- [21] Zhou J, Zhang S, Ong CN, Shen HM. Critical role of pro-apoptotic Bcl-2 family members in andrographolide-induced apoptosis in human cancer cells. *Biochem Pharmacol* 2006;72:132–44.
- [22] Liu CJ, Hwang JM, Wu TT, Hsieh YH, Wu CC, Hsieh YS, et al. Anion exchanger inhibitor DIDS induces human poorly-differentiated malignant hepatocellular carcinoma HA22T cell apoptosis. *Mol Cell Biochem* 2008;308:117–25.
- [23] Shen H, Yang C, Liu J, Ong C. Dual role of glutathione in selenite-induced oxidative stress and apoptosis in human hepatoma cells. *Free Radic Biol Med* 2000;28:1115–24.
- [24] Ying S, Hacker G. Apoptosis induced by direct triggering of mitochondrial apoptosis proceeds in the near-absence of some apoptotic markers. *Apoptosis* 2007;12:2003–11.
- [25] Won YK, Ong CN, Shen HM. Parthenolide sensitizes ultraviolet (UV)-B-induced apoptosis via protein kinase C-dependent pathways. *Carcinogenesis* 2005;26:2149–56.
- [26] Pistritto G, Puca R, Nardinocchi L, Sacchi A, D'Orazi G. HIPK2-induced p53Ser46 phosphorylation activates the KILLER/DR5-mediated caspase-8 extrinsic apoptotic pathway. *Cell Death Differ* 2007;14:1837–9.
- [27] Liu X, Yue P, Khuri FR, Sun SY. p53 upregulates death receptor 4 expression through an intronic p53 binding site. *Cancer Res* 2004;64:5078–83.
- [28] Li H, Zhu H, Xu CJ, Yuan J. Cleavage of BID by caspase 8 mediates the mitochondrial damage in the Fas pathway of apoptosis. *Cell* 1998;94:491–501.
- [29] Luo X, Budihardjo I, Zou H, Slaughter C, Wang X. Bid, a Bcl2 interacting protein, mediates cytochrome c release from mitochondria in response to activation of cell surface death receptors. *Cell* 1998;94:481–90.
- [30] Hsu YT, Youle RJ. Bax in murine thymus is a soluble monomeric protein that displays differential detergent-induced conformations. *J Biol Chem* 1998;273:10777–83.
- [31] Nechushtan A, Smith CL, Hsu YT, Youle RJ. Conformation of the Bax C-terminus regulates subcellular location and cell death. *EMBO J* 1999;18:2330–41.
- [32] Miura M, Friedlander RM, Yuan J. Tumor necrosis factor-induced apoptosis is mediated by a CrmA-sensitive cell death pathway. *Proc Natl Acad Sci USA* 1995;92:8318–22.
- [33] Kuo PL, Hsu YL, Lin TC, Lin LT, Lin CC. Induction of apoptosis in human breast adenocarcinoma MCF-7 cells by prodelphinidin B-2 3,3'-di-O-gallate from *Myrica rubra* via Fas-mediated pathway. *J Pharm Pharmacol* 2004;56:1399–406.
- [34] Huang Q, Shen HM, Ong CN. Inhibitory effect of emodin on tumor invasion through suppression of activator protein-1 and nuclear factor-kappaB. *Biochem Pharmacol* 2004;68:361–71.
- [35] Takeda K, Stagg J, Yagita H, Okumura K, Smyth MJ. Targeting death-inducing receptors in cancer therapy. *Oncogene* 2007;26:3745–57.
- [36] Cretney E, Takeda K, Smyth MJ. Cancer: novel therapeutic strategies that exploit the TNF-related apoptosis-inducing

- ligand (TRAIL)/TRAIL receptor pathway. *Int J Biochem Cell Biol* 2007;39:280–6.
- [37] Voortman J, Resende TP, Abou El Hassan MA, Giaccone G, Kruyt FA. TRAIL therapy in non-small cell lung cancer cells: sensitization to death receptor-mediated apoptosis by proteasome inhibitor bortezomib. *Mol Cancer Ther* 2007;6:2103–12.
- [38] Ridgway PJ, Hale TK, Braithwaite AW. p53 confers a selective advantage on transfected HeLa cells. *Oncogene* 1993;8:1069–74.
- [39] Haupt Y, Rowan S, Oren M. p53-mediated apoptosis in HeLa cells can be overcome by excess pRB. *Oncogene* 1995;10:1563–71.
- [40] Singh M, Sharma H, Singh N. Hydrogen peroxide induces apoptosis in HeLa cells through mitochondrial pathway. *Mitochondrion* 2007;7:367–73.
- [41] Micheau O, Lens S, Gaide O, Alevizopoulos K, Tschopp J. NF-kappaB signals induce the expression of c-FLIP. *Mol Cell Biol* 2001;21:5299–305.
- [42] Thome M, Tschopp J. Regulation of lymphocyte proliferation and death by FLIP. *Nat Rev Immunol* 2001;1:50–8.
- [43] Yi X, Yin XM, Dong Z. Inhibition of Bid-induced apoptosis by Bcl-2. tBid insertion, Bax translocation, and Bax/Bak oligomerization suppressed. *J Biol Chem* 2003;278:16992–9.